NASA Technical Memorandum 83621

Reducing Numerical Diffusion for Incompressible Flow Calculations

R.W. Claus and G.M. Neely
Lewis Research Center
Cleveland, Ohio

S.A. Syed
United Technologies
Pratt & Whitney Aircraft Group
East Hartford, Connecticut

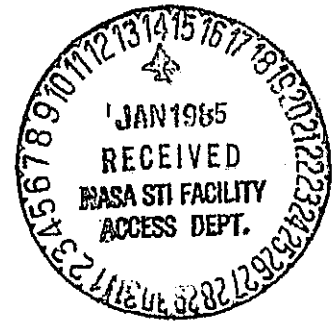

Prepared for the
Western States Meeting of the Combustion Institute
Boulder, Colorado, April 2-3, 1984

NASA

REDUCING NUMERICAL DIFFUSION FOR INCOMPRESSIBLE FLOW CALCULATIONS

R.W. Claus and G.M. Neely
National Aeronautics and Space Administration
Lewis Research Center
Cleveland, Ohio 44135

and

S.A. Syed
United Technologies
Pratt & Whitney Aircraft Group
East Hartford, Connecticut

SUMMARY

A number of approaches for improving the accuracy of incompressible, steady-state flow calculations are examined. Two improved differencing schemes, Quadratic Upstream Interpolation for Convective Kinematics (QUICK) and Skew-Upwind Differencing (SUD), are applied to the convective terms in the Navier-Stokes equations and compared with results obtained using hybrid differencing. In a number of test calculations, it is illustrated that no single scheme exhibits superior performance for all flow situations. However, both SUD and QUICK are shown to be generally more accurate than hybrid differencing.

INTRODUCTION

Three-dimensional calculations of combustor flow fields are currently imposing severe demands on the computer hardware capabilities and computing budgets of gas turbine manufacturers. One of the main reasons for this relates to the large number of complex physical processes occurring in the combustor. Airflow, fuel spray, reaction kinetics, flame radiation, and turbulence must be modeled and the related differential equations solved. Obtaining accurate solutions to these modeled equations entails overcoming another difficulty. Current combustor codes are, generally, based on the SIMPLE algorithm developed by Patankar and Spalding (ref. 1). Frequently used in conjunction with this solution algorithm is hybrid differencing to approximate the convective terms in the governing equations. In most practical calculations this results in the use of first order accurate upwind differencing for most of the flow field. The overly dissipative solutions obtained can mask important flow field features (ref. 2). Ideally, this can be overcome through the use of additional grid points. In three dimensional calculations, however, this soon becomes impractical due to the large number of physical processes that must be modeled.

To alleviate this problem, NASA has initiated a program to identify and incorporate an improved accuracy differencing scheme into a combustor performance code. Under a portion of this program a competitive contract was awarded to United Technologies (with A.D. Gosman as consultant) to examine and implement a variety of improved accuracy differencing schemes. The schemes examined include Quadratic Upstream Interpolation for Convective Kinematics (QUICK) and variants of Skewed-Upwind Differencing (SUD). The variants of SUD involve different procedures to ensure that nonphysical oscillations do not occur in the solution.

The purpose of this paper is to draw some general conclusions concerning the accuracy of the convective differencing schemes studied. A number of non-turbulent test calculations are made to illustrate the accuracy and stability (convergence) characteristics of the various schemes. In general, these test calculations indicate that both QUICK and SUDS are more accurate than hybrid differencing although these schemes greatly slow convergence of the governing equations.

MATHEMATICAL FORMULATION

The numerical code employed in this study provides the capability to analyze steady-state, two-dimensional, elliptic, turbulent flows. Only the pertinent features of the code shall be reviewed here as further details are available in the open literature.

The governing equations, written in tensor notation, include:

$$\text{Continuity} - \frac{\partial U_i}{\partial x_i} = 0 \tag{1}$$

$$\text{Momentum} - \underbrace{U_i \frac{\partial U_j}{\partial x_i}}_{\text{Convection}} = \underbrace{-\frac{1}{\rho}\frac{\partial P}{\partial x_j}}_{\substack{\text{Pressure} \\ \text{gradient}}} + \underbrace{\frac{\partial}{\partial x_i}\left(\nu \frac{\partial U_j}{\partial x_i}\right)}_{\text{Diffusion}} \tag{2}$$

The numerical code used in these studies can solve the two additional equations relating to the turbulence model of reference 3. However, the test calculations are meant to focus on the accuracy with which the momentum equations can be solved, therefore, the viscosity was fixed at a laminar value.

The governing equations are discretized through integral analysis or the "finite volume" method following the procedure of Gosman and Lai, (ref. 4). Integrals across each computational cell face are evaluated using the Mean Value Theorem on the grid illustrated in figure 1(a). Approximations for the convective and diffusive terms are then made depending on the differencing procedure used. The pressure gradient and diffusive terms are central differenced while the differencing of the convective terms will be noted in the next section. The resulting fluxes across each cell face are then summed. This equation when arranged into a substitution formula for the variable being solved (for example ϕ_p is the variable being solved for at point P) becomes:

$$a_p \phi_p = \sum_W a_i \phi_i + Su \tag{3}$$

where $\sum_W$ denotes summation of the neighbors of P.

CONVECTIVE DIFFERENCING

Hybrid Differencing

The practice most commonly used, at present, is to employ hybrid differencing to approximate the convective terms. This involves the use of second order accurate central differencing when the cell Peclet number (Pe_c) is less than an absolute value of 2, while first order accurate upwind differencing is used when $|Pe_c| > 2$. The major advantage of this scheme is the unconditionally bounded or oscillation free solutions it provides.

For example, if solving for ϕ on the staggered grid (fig. 1(a)), one of the convective terms becomes:

$$\frac{\partial u\phi}{\partial x} = \frac{(u\phi)_e - (u\phi)_w}{\Delta x} \tag{4}$$

where for central differencing (uniform grid spacing) -

$$(u\phi)_e = \frac{1}{2} u_e(\phi_E + \phi_P)$$

$$(u\phi)_w = \frac{1}{2} u_w(\phi_W + \phi_P)$$

for upwind differencing ($u > 0$) -

$$(u\phi)_e = u_e\phi_P$$

$$(u\phi)_w = \frac{1}{2} u_w(\phi_W + \phi_P)$$

QUICK Differencing

This scheme, developed by Leonard (ref. 5), is second order accurate and not unconditionally bounded. (The scheme may produce nonphysical oscillations in the solution.) It approximates convective terms using an upstream biased quadratic interpolation. For example, using the grid in figure 1(b) and approximating equation (4) as before:

For $u > 0$

$$(u\phi)_e = U_e \left\{ -\frac{1}{8}\phi_W + \frac{3}{4}\phi_P + \frac{3}{8}\phi_E \right\}$$

$$(u\phi)_w = U_w \left\{ -\frac{1}{8}\phi_{WW} + \frac{3}{4}\phi_W + \frac{3}{8}\phi_P \right\}$$

Skew Upwind Differencing (SUD)

This scheme, developed by Raithby (ref. 6), is first order accurate and, as with QUICK, is not unconditionally bounded. While SUD is formally the same order accuracy as upwind differencing, its truncation error is less than upwind.

SUD attains this higher accuracy by differencing in an upwind manner along the flow streamlines. Each streamline is defined by the velocity vector at each grid boundary (fig. 1(c)). The upstream value of the variable to be calculated is then obtained by a back projection of the velocity vector and simply interpolating between the two neighboring values. For example, using the grid of figure 1(c) and solving equation (4) as in the previous two examples:

For $u > 0$ and $v > 0$

$$(u\phi)_e = u_e \phi_P$$

$$(u\phi)_w = u_w (1 - \alpha) \phi_W + u_w \alpha \phi_{SW}$$

where

$$\alpha = \text{minimum of } (1, v/2u)$$

Flux Blending

The concept of flux-blending is analogous to the "Flux Corrected Transport" (FCT) technique of Boris and Books (ref. 7). The procedures employed here were developed by Gosman, Lai, and Peric and are detailed in reference 8. In general, the flux blended schemes employ a weighted mean of a bounded (but low order accuracy) differencing scheme and an unbounded, more accurate scheme. The main factor is to blend as little of the lesser accurate scheme as possible while still maintaining a properly bounded solution. The two differencing schemes blended involve upwind differencing and the more accurate SUD.

BSUDS1

This procedure, "Bounded Skew Upwind Differencing Scheme 1" blends upwind and SUD in proportions sufficient to suppress negative coefficients in equation (3). This is a sufficient condition for a bounded solution, however, it tends to be more dissipative than necessary.

BSUDS2

This procedure "Bounded Skew Upwind Differencing Scheme 2" blends upwind and SUD in proportions ensuring that when negative coefficients occur, their contribution is below the level that would cause the solution to be physically unrealistic. This procedure is iterative and starts from an initial, totally skew differenced estimate. If the calculated variable has a value no greater or lesser than that of its neighbors, then the solution is bounded and no blending is performed. If the solution is out of the range of neighboring values, then blending is performed. In the extreme, this blending would result in upwind differencing. The use of neighboring values as limits in determining the "boundedness" of the solution is only valid when the equation being solved lacks source terms. However, the momentum equations contain significant source contributions. The implications of this are still being studied, but the results reported in later sections shall demonstrate that the use of neighboring values as physical limits provides highly accurate results.

This bounding procedure, while simple in concept, is difficult to apply to an iterative solution scheme. If an initial SUD calculation was made and then the coefficients were updated for bounding and the equation solved a second time, the computational time required for one iteration would be approximately doubled. To reduce this computational overhead BSUDS2 calculations were typically restarted from a BSUDS1 calculation with the bounding evaluated based on the previous iteration values. This results in some "unboundedness" when the equations are not fully converged, however, the final result should be bounded.

Solution Algorithm

As solution algorithm for solving the governing equations will be only briefly reviewed here (refs. 4 and 9) are strongly recommended for further details.

Once the momentum equations are approximated on the staggered grid, these equations must be solved in a process insuring that all governing equations are satisfied. In the SIMPLE algorithm, each momentum equation is sequentially solved using a guessed or old pressure field from the previous iteration. A pressure correction equation is then solved and the values of velocity and pressure are revised to more closely satisfy continuity. Iteration on this procedure is then continued until all equations are satisfied to a low normalized residual level (typically 10^{-2} or 10^{-4} for the calculations herein reported).

Scalar Transport Test Calculation

Following the procedure detailed in reference 8, a preliminary assessment of the accuracy associated with the various differencing schemes was made solving the following scalar transport equation:

$$\frac{\partial U\phi}{\partial x} + \frac{\partial V\phi}{\partial y} = 0$$

for

U = constant

V = constant = $U \tan \theta$

where

θ = flow angle

A normal distribution of ϕ was imposed along a streamline centered coordinate (fig. 2). This provided the boundary conditions for ϕ and a single point (ϕ_p) calculation could then be made using the differencing schemes described earlier.

RESULTS AND DISCUSSION

The accuracy of the previously described convective differencing schemes is illustrated through a series of test calculations. The first test problem is a single cell calculation of scalar transport. Following this example a variety of laminar flow calculations are made to examine whether the conclusions that were drawn from the scalar calculation remain valid for the full momentum equations. The effect that each of these schemes has on convergence is examined in the final section.

Scalar Transport Test Calculation

A straight-forward approach to study the accuracy of various differencing schemes is to solve an equation describing the transport of a scalar with no diffusion or source terms. This problem has been described in the previous section and is graphically illustrated (fig. 2). The exact answer to this problem is that the scalar, ϕ, remains equal to 1.0 along the streamline intersecting point P.

Solutions for the scalar transport equation as a function of flow angle for the various differencing schemes are displayed in figure 3. All schemes agree with the exact solution at a flow angle of zero, but departing from this each scheme displays some degree of error relating to numerical smearing or diffusion. Upwind differencing displays the greatest amount of numerical diffusion with the largest errors occurring at 45°. QUICK displays a similar behavior but the overall level of error is much less. SUD displays an error maximum around 15° but tends to zero at angles approaching 45°. BSUDS1 displays more error than SUD with a maximum error around 22°. All the first order schemes, upwind, SUD, and BSUDS1, display similar error levels for flow angles less than about 5° although these errors are generally small. QUICK displays superior performance to the best of the first order schemes, SUD, at flow angles up to about 15°. Above a flow angle of 15° SUD is generally more accurate than any of the other schemes.

The penalty to be paid for ensuring against nonphysical oscillations using the first flux blending scheme can be seen by comparing the SUD and BSUDS1 results in figure 3. (The first flux blending scheme requires that all advection coefficients (eq. (3)) be positive as detailed in the earlier section.) For example, at 30° BSUDS1 displays about 6 percent error while SUD displays less than one percent. The BSUDS2 scheme is not readily suitable to test this problem, but logically one can expect this scheme to exhibit an accuracy between SUD and BSUDS1.

It is important to note that these test calculations were made on a uniformly spaced grid. The accuracy of the SUD calculations would change as the cell aspect ratio ($\Delta X/\Delta Y$) was varied. Figure 4 displays an example of how cell aspect ratio affects the accuracy of SUD. (This figure is shown for illustration purposes only - the indicated accuracy is dependent on the formulation of the scalar calculation.) For increasing aspect ratios above 1, SUD is more accurate at flow angles only slightly skewed to the grid. For example, at a cell aspect ratio of 2, SUD has an optimal performance around a flow angle of 26°. At an aspect ratio of 1, the best performance of SUD is around 45°.

Due to the impact of cell aspect ratio on SUD accuracy all of the test calculations were made on a uniform mesh or the mesh was uniform in the important flow regions and allowed to be nonuniform only far downstream.

Laminar Flow Test Calculations

To examine whether the scalar calculations remain a valid test of convective accuracy when the full momentum equations are solved, a series of laminar flow calculations were made. Laminar test calculations were chosen over turbulent flow calculations due to the fact that numerical inaccuracy should exhibit itself as numerical smearing. The diffusion added by a turbulence model would obsecure the differences in convective accuracy. In laminar flow calculations the more accurate solutions will display steeper velocity gradients.

Driven Cavity Test Calculations

The first laminar flow calculation is of the driven cavity flow field. This geometry is frequently used to assess numerical accuracy (refs. 10 to 13). Fine grid calculations (refs. 11 and 12) are available as a "standard" for accuracy comparisons. Figure 5 displays a typical flow field calculation for this geometry. The moving upper wall (not shown) imposes a circulation in the cavity. The calculations were made for a Reynold's number of 1000 based on cavity height. The grid points in these calculations were uniformly spaced.

Calculated velocity profiles through the center of the circulation vortex are shown in figure 6. In this figure the results of progressively finer grids are compared against the "standard". The hybrid results are slowly tending toward the more accurate results and yet, even the 80 by 80 calculations exhibit numerical inaccuracy.

The velocity peak seen in figure 6 around $Y/L = 0.2$ is used as a measure of accuracy in figure 7. Although it is difficult to quantify the accuracy of an entire two-dimensional flow field by a single point, this point does seem representative of the accuracy. In figure 7 the velocity peak is shown versus the number of grid points used in the hybrid, QUICK, and BSUDS2 calculations. The line at $U/Uw = 0.4$ indicates the "standard" result. The QUICK results indicate a strong response to grid refinement such that at 6400 grid points the QUICK results match the "standard". The first order schemes hybrid and BSUDS2 appear to be highly inaccurate with the 6400 grid point calculations being only as accurate as the 400 grid point calculations of QUICK.

The poor performance of the BSUDS2 calculations is surprising in view of the scalar calculations previously shown. Calculations were made using unbounded SUD and were found to be indistinguishable from the BSUDS2 calculations. Therefore, the flux blended procedure can not account for the poor performance.

Laminar Flow Calculations With Various Inlet Flow Angles

A second series of laminar flow calculations were made to further explore the flow angle/accuracy dependance. The geometry employed in these calculations is shown in figure 8. The inlet flow angle was varied from 40 to 0°.

All calculations were for a Reynold's number of 1000 based on inlet height. Grid points were arranged with uniform spacing in the forward portion of the flow field (aspect ratio equal to 1) while the mesh was nonuniform far downstream.

Inlet Flow Angle of 40°

Calculations made with two different grid meshes are shown for a X/H of 0.5 in figure 9. The coarse mesh calculations (fig. 9(a)) show that both QUICK and BSUDS2 provide steeper gradients than the hybrid calculation. The BSUDS2 results appear to be overall more accurate especially when these results are compared to the fine mesh calculations (fig. 9(b)). The fine mesh calculations (fig. 9(b)) again display the poor performance of hybrid differencing and the higher accuracy of QUICK and BSUDS2. In contrast to the coarse mesh results QUICK and BSUDS2 appear to be of nearly similar accuracy.

The performance of BSUDS1 and BSUDS2 for the fine mesh calculations can be seen in figure 9(c). The results for these schemes are quite similar with the BSUDS2 exhibiting slightly steeper velocity gradients, and thereby slightly greater accuracy. On a coarse mesh (not shown) the results were similar.

Inlet Flow Angle of 25°

Velocity profiles at X/H = 0.5 for an inlet flow angle of 25° are displayed in figure 10. The coarse grid results (fig. 10(a)) indicates that hybrid differencing again smears the velocity profile more than the QUICK or BSUDS2 results. The fine mesh results (fig. 10(b)) indicate smaller differences between all three schemes. The hybrid calculation smears the velocity profile more than the other two calculations, but the indicated error is less than that in the 40° test calculations of figure 9. The QUICK results exhibit a nonphysical oscillation in the velocity profile around Y/H = 0.5 while the BSUDS2 result displays a smooth but accurate velocity profile.

The comparison between the BSUDS1 and the BSUDS2 calculations is displayed in figure 10(c). The results are similar to the 40° comparison (fig. 9(c)) with BSUDS2 displaying only slightly improved accuracy. This result is surprising in light of the scalar calculations of figure 3. In those calculations there was a large variation in accuracy between BSUDS1 and BSUDS2 at the two different flow angles. This will be more fully discussed in the summary section.

Inlet Flow Angle of 0°

Velocity profiles at X/H = 1.0 for an inlet flow angle of 0° are displayed in figure 11. Both the coarse mesh results (fig. 11(a)) and the fine mesh results (fig. 11(b)) show very little effect of the convective operator. This is expected since the scalar transport test calculations indicated that all schemes are essentially exactly correct for a 0° flow angle.

Summary of Accuracy Tests

From the series of flow calculations made, no single differencing scheme displayed superior accuracy in all calculations. The scalar calculation demonstrated that performance of the differencing scheme was related to flow angle. The laminar flow calculations indicated that other factors must be equally important. For instance, a possible explanation of the relatively poor performance of BSUDS2 in the driven cavity calculation versus the other flow calculations can be advanced from consideration of the gradients in the calculated variable. In the inclined inlet flow calculations, the linear variation of velocity issuing from the inlet can be well represented by any form of SUD. The normal distribution used in the scalar calculations can also be fairly accurately accommodated by SUD. The driven cavity exhibits velocity gradients which are dissimilar to either of the previous examples. The moving wall establishes a steep velocity gradient which can, apparently, only be fairly well represented by QUICK. However this driven cavity calculation may be somewhat unrepresentative of combustor-type geometries. The inclined inlet flow field has features that are highly similar to combustors, suggesting that SUD can be used in combustor calculations to provide some improved accuracy.

Convergence Tests

Computational times to converge the system of governing equations is shown in table I for three different convective schemes. These calculations were all made on a Cray 1s using the SIMPLE algorithm for the driven cavity flow geometry. In general, either BSUDS2 or QUICK required more time to converge than hybrid. The slowest performer was QUICK with times in the range of three to five times slower to converge than hybrid differencing. BSUDS2 was usually only slightly slower than hybrid. The other variants of SUD gave results comparable to the BSUDS2 timings. It should be noted that the choice of underrelaxation has a strong influence on the convergence rate and that the highest under-relaxation that would promote stable convergence was used. However, extensive optimization was not done and it may be possible to achieve slightly faster or slower convergence times.

CONCLUSIONS

1. The accuracy of BSUDS2 and QUICK was generally greater than hybrid differencing for the series of calculations reported here. In the driven cavity series of calculations BSUDS2 was about as inaccurate as hybrid differencing while QUICK displayed a high level of accuracy. In a series of calculations more representative of combustor-type geometries (inclined inlet), BSUDS2 and QUICK were highly accurate while hybrid differencing was very inaccurate.

2. The bounding procedure used in BSUDS2 produced solutions free of nonphysical oscillations while maintaining a high level of accuracy.

3. Both QUICK and SUD generally required more time to converge than the hybrid calculations. This became more pronounced in fine mesh calculations.

ACKNOWLEDGMENTS

The author would like to acknowledge the insights provided by A.D. Gosman and M. Peraic of Imperial College.

REFERENCES

1. Patankar, S.V. and Spalding, D.B.: Int. J. Heat Mass Transfer 15, 1787 (1972).

2. Claus, R.W.: Analytical Calculation of a Single Jet in Crossflow and Comparison With Experiment, NASA TM-83027, 1983.

3. Jones, W.P., and Launder, B.E.: Int. J. Heat Mass Transfer 15, 301 (1972).

4. Gosman, A.D. and Lai, K.Y.: Finite Difference and Other Approximations for the Transport and Navier-Stokes Equations, Fluids Section, Mechanical Engineering Depart nt, Imperial College, London SW7 FS/82/18.

5. Leonard, B.P.: Comput. Methods Appl. Mech. Eng. 19, 59 (1979).

6. Raithby, G.D.: Comput. Methods Appl. Mech. Eng. 9, 153 (1976).

7. Boris, J.P. and Book, D.L.: J. Comput. Phys. 11, 38 (1973).

8. Syed, S.A., Chiapetta, L.M., and Gosman, A.D., "Error Reduction Program, Final Report," NASA CR-174776, 1985.

9. Patankar, S.V.: Numerical Heat Transfer and Fluid Flow, Hemisphere Publishing Corporation, 1980.

10. Burggraf, O.R.: "Analytical and Numerical Studies of the Structure of Steady Flows," Journal of Fluid Mech., Vol. 24, 1966.

11. Rubin, S.G., Khosla, P.K., "Polynomial Interpolation Methods for Viscous Flow Calculations," Journal of Computational Physics, Vol. 24, 1977.

12. Gosman, A.D., Issa, R.I., "Computational Fluid Dynamics and Heat/Mass Transfer: An Introductory Survey Course," Lecture notes for a course given at Penn State University, June 1983.

13. Staff Langley Research Center, "Numerical Studies of Incompressible Viscous Flow in a Driven Cavity," NASA SP-378, 1975.

TABLE I. - CONVERGENCE TIMES FOR THREE CONVECTIVE DIFFERENCING SCHEMES USING THE SIMPLE ALGORITHM. DRIVEN CAVITY FLOW CALCULATIONS

Number of nodes	Hybrid	BSUDS2	QUICK
	CPU time, sec		
100	6.1	11.9	7.6
400	17.5	18.0	47.1
1600	118.5	118.2	524.7
6400	1019.2	1517.6	5551.0

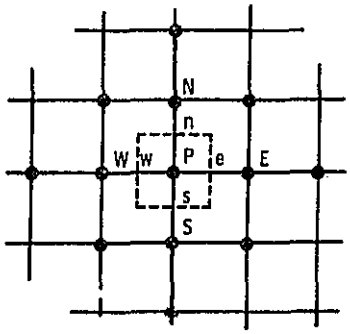

(a) Staggered grid system used for hybrid differencing.

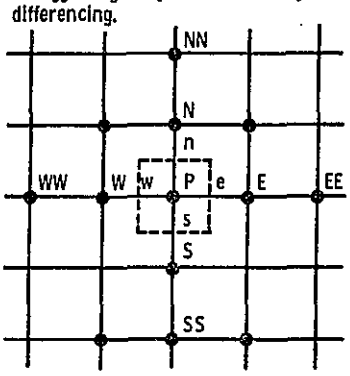

(b) Grid system used with QUICK differencing.

Figure 1. - Grid structures used with various convective differencing schemes.

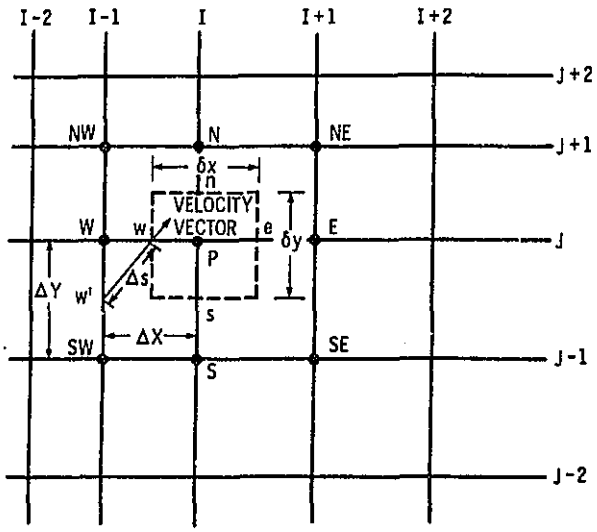

(c) Grid system used with SKEW differencing.

Figure 1. - Concluded.

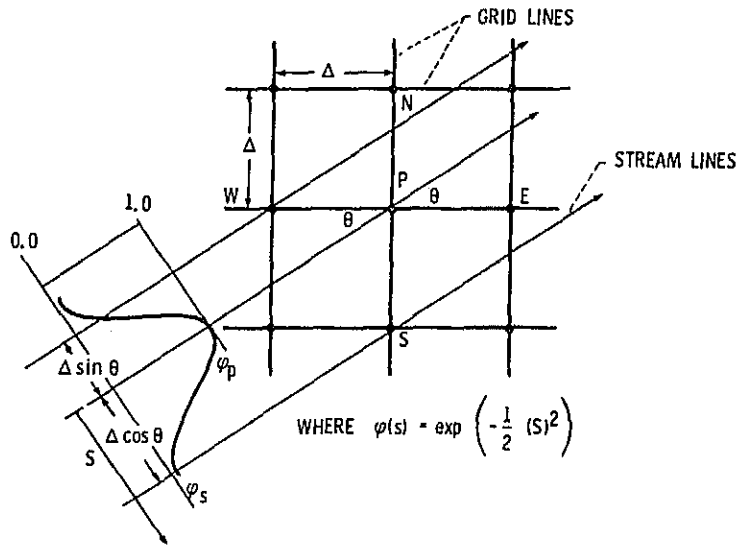

Figure 2. - Illustration of the scalar transport test calculation.

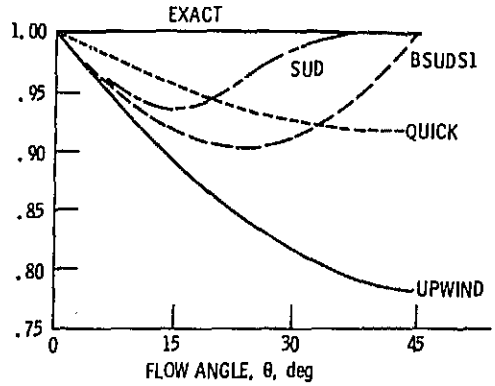

Figure 3. - Results of the scalar transport test calculations shown versus flow angle.

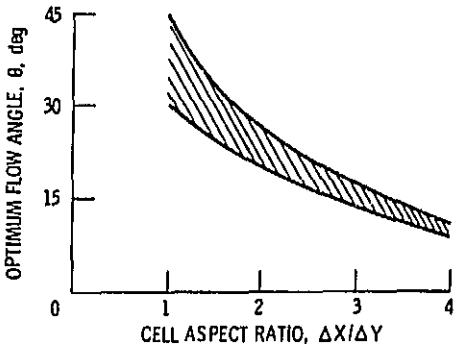

Figure 4. - Optimum flow angle for skew differencing (SUD) shown for various computational cell aspect ratios. Shaded region indicates approximately less than one percent inaccuracy in solution of scalar transport test calculation.

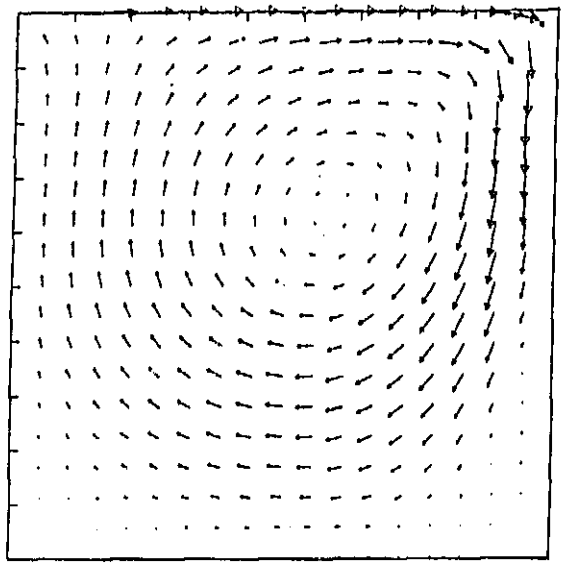

Figure 5. - Velocity vectors for a typical driven cavity calculation. The upper moving wall is removed from the plot. Flow Re = 1000.

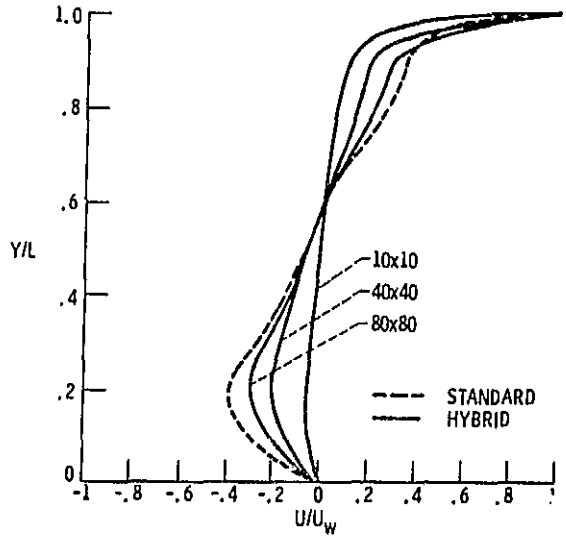

Figure 6. - Velocity profiles through the center of the circulation vortex for the driven cavity calculations. Shown are the results of hybrid calculations compared with high accuracy "standard" results.

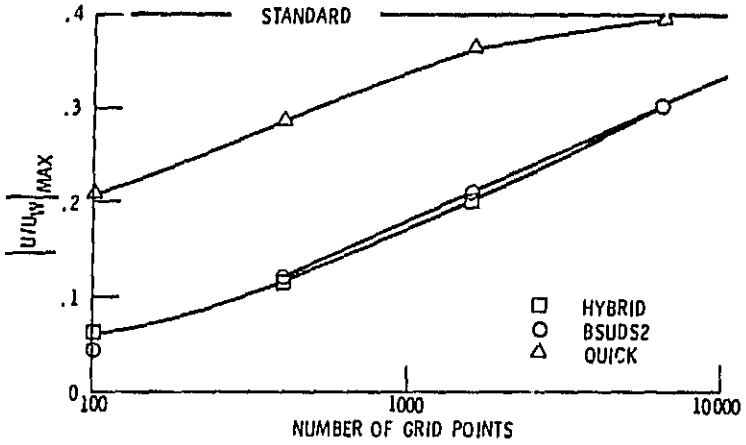

Figure 7. - Velocity peak value plotted against number of grid points for the driven cavity flow calculations.

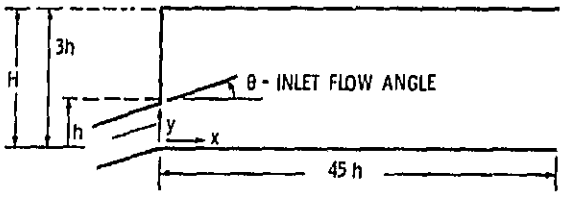

Figure 8. - Geometry illustration for laminar flow calculations employing various inlet flow angles.

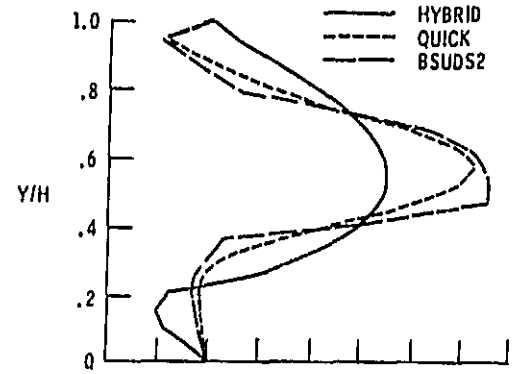

(a) Coarse grid (30x22) calculations comparing hybrid, QUICK and BSUDS2.

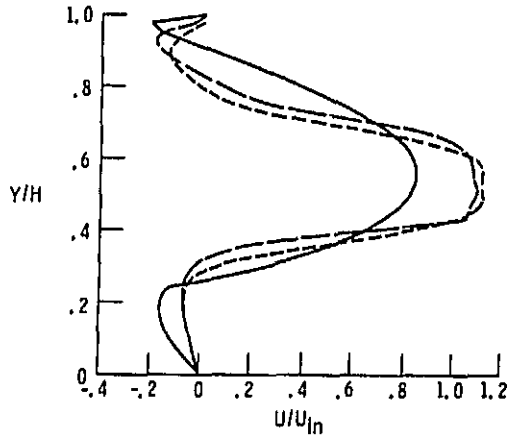

(b) Fine grid (58x38) calculations comparing hybrid, QUICK and BSUDS2.

Figure 9. - Laminar flow test calculations with inlet flow angle of 40°; geometry of figure 8.

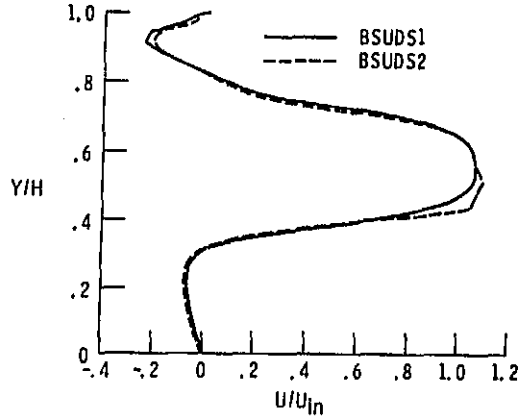

(c) Fine grid (58x38) calculations comparing BSUDS1 and BSUDS2.

Figure 9. - Concluded.

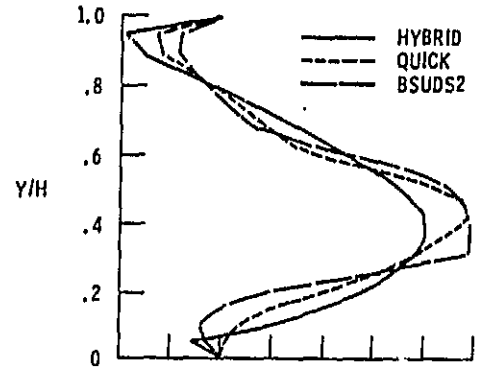

(a) Coarse grid (30x22) calculations.

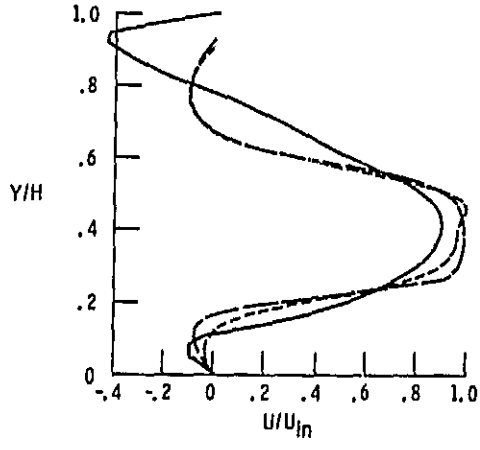

(b) Fine grid (58x38) calculations.

Figure 10. - Laminar flow test calculations comparing hybrid, QUICK and BSUDS2. Inlet flow angle of 25°; geometry of figure 8. X/H = 0.5.

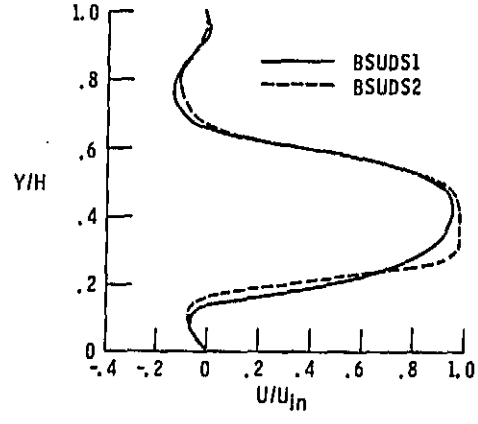

(c) Fine grid (58x38) calculations comparing BSUDS1 and BSUDS2.

Figure 10. - Concluded.

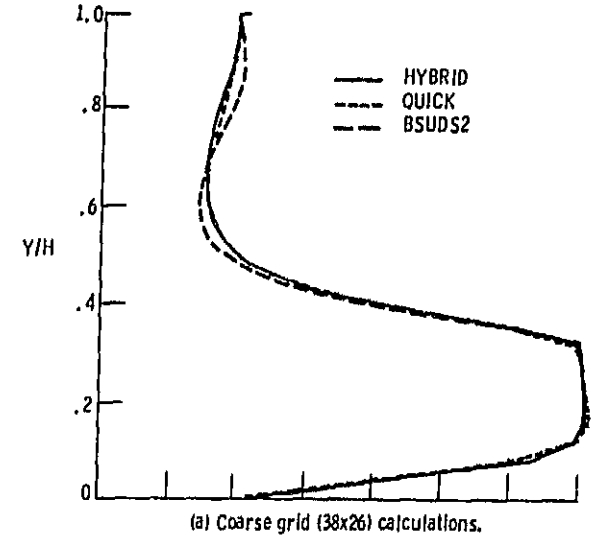

(a) Coarse grid (38x26) calculations.

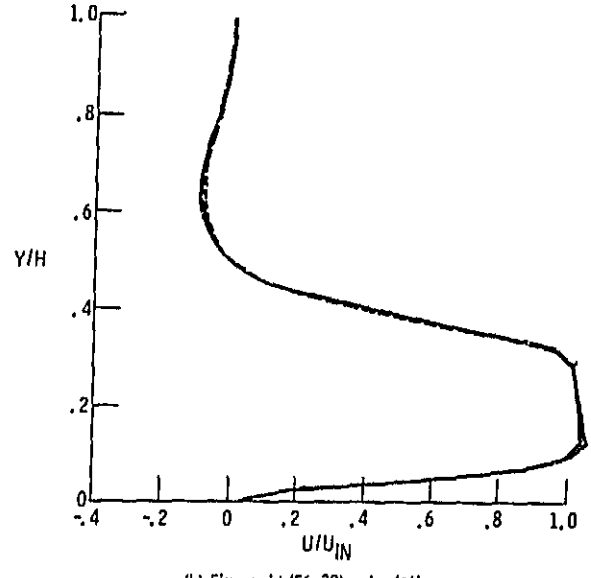

(b) Fine grid (56x38) calculations.

Figure 11. - Laminar flow test calculations comparing hybrid, QUICK, and BSUDS2. Inlet flow angle, 0^{0}; geometry of figure 8.